frontiers | Frontiers in Forests and Global Change

TYPE Original Research
PUBLISHED 27 March 2025
DOI 10.3389/ffgc.2025.1531983

OPEN ACCESS

EDITED BY
Xianliang Zhang,
Hebei Agricultural University, China

REVIEWED BY
Liangjun Zhu,
Central South University Forestry and Technology, China
Jingwen Yang,
Southwest Forestry University, China

*CORRESPONDENCE
Dongyou Zhang
✉ zhangdy@hrbnu.edu.cn

RECEIVED 22 November 2024
ACCEPTED 12 March 2025
PUBLISHED 27 March 2025

CITATION
Wang X, Wang Z, Zhang D, Yu S, Zhang T, Luo T, Li X, Du B and Cheng X (2025) Response of *Pinus sylvestris* var. *mongholica* tree-ring density to climatic factors in Northeast China under climate warming background.
Front. For. Glob. Change 8:1531983.
doi: 10.3389/ffgc.2025.1531983

Response of *Pinus sylvestris* var. *mongholica* tree-ring density to climatic factors in Northeast China under climate warming background

Xinrui Wang[1], Zhaopeng Wang[1], Dongyou Zhang[1,2,3]*, Shulong Yu[4], Tongwen Zhang[4], Taoran Luo[1], Xiangyou Li[1], Bingyun Du[1] and Xiyao Cheng[1]

[1]Heilongjiang Province Key Laboratory of Geographical Environment Monitoring and Spatial Information Service in Cold Regions, Harbin Normal University, Harbin, China, [2]Heilongjiang Wuyiling Wetland Ecosystem National Observation and Research Station, Yichun, China, [3]Wuyiling Wetland Ecosystem Observation and Research Station of Heilongjiang Province, Yichun, China, [4]Key Laboratory of Tree-ring Physical and Chemical Research of China Meteorological Administration, Xinjiang Laboratory of Tree Ring Ecology, Institute of Desert Meteorology, China Meteorological Administration, Ürümqi, China

Under the background of increasing global climate change, understanding the impact of climate variables on forest ecosystems has become an important topic in ecology and climatology. To explore the connection between tree-ring density and climatic variables, *Pinus sylvestris* var. *mongholica* (Ps) trees growing at the northwestern foot of the Greater Khingan Mountains (GKM) were selected as research subjects. Correlations between their density index and climatic factors were analyzed using the basic theory and methods of dendrochronology. The impacts of either climatic variable (temperature and precipitation) on the tree-ring density and growth of Ps were also analyzed under warming conditions. Results showed that the tree ring width index (TRW) was positively correlated with the earlywood width index (EW), latewood width index (LW), minimum density (MND), density of earlywood (EWD), maximum density (MXD), and density of latewood (LWD) (all at $p < 0.01$). These results imply that the inter-annual changes of the three groups of indicators exhibit a high degree of synchronization. The analysis of the density index to climatic variables showed that the density index of different growth rings of Ps was considerably affected by temperature and precipitation. Both TRD and EWD showed a positive correlation with maximum temperature in May, while LWD and MXD showed a positive correlation with precipitation in March. However, EWD as well as MND showed a considerably negative correlation with temperature in the previous autumn and likewise with precipitation in spring and summer. The results obtained from a follow-up redundancy analysis further validated those above from the response function analysis. The sliding correlation analysis indicated that the dynamic stability of the ring density index became stronger or weaker over time. This study reveals the response differences of the ring density indices of Ps to climate factors and their temporal stability, which is helpful to understand the

response relationship between conifer species growth and climate in northern GKM.

KEYWORDS

climatic element, *Pinus sylvestris* var. *mongholica*, trees grow, tree-ring density, Northeast China

1 Introduction

Global warming has become a paramount environmental concern, continually affecting human activities and impairing the stability of the Earth's ecosystem. According to the Sixth Assessment Report of the IPCC, the average temperature increased by 1.1°C between 2000 and 2020 when compared to 1850–1900 (Kikstra et al., 2022). The high latitudes of the Northern Hemisphere have experienced substantial warming during the past 150 years, but especially from the 1980s onward (Smerdon et al., 2013). As a crucial component of the terrestrial ecosystem, forests have incurred substantial impacts on their structure and function due to climate warming (Van Mantgem et al., 2009; Anderegg et al., 2022). As a fundamental dimension of forests, tree growth is not only influenced by intrinsic factors but also closely related to climatic conditions (Liang et al., 2023). Although a longer tree growing season driven by climate warming may favor stem radial growth (Yang et al., 2017), the rising frequency of extreme climate events like droughts is leading to large-scale forest declines (Chen et al., 2017). To understand the relationship between tree growth and climate factors, it is necessary to obtain long-term data of different tree ring indicators (Li et al., 2024). By revealing the response relationship of different tree ring indicators to climate factors, the possible impacts of climate change on tree growth and forest ecosystem can be clarified, thus providing scientific basis for forest management and management (Singh et al., 2024).

Tree-ring data constitute an unparalleled paleoclimatic proxy due to their precise annual resolution, spatiotemporal continuity, and hemispheric-scale coverage (Fritts, 1991; Zhang et al., 2011a; Wang et al., 2016; Esper et al., 2020). Tree-ring data constitute an unparalleled paleoclimatic proxy due to their precise annual resolution, spatiotemporal continuity, and hemispheric-scale coverage (Bouriaud et al., 2005; Camarero and Gutiérrez, 2017). Throughout the radial expansion of trees, the generation, expansion of cells, and formation of cell walls are jointly influenced by climatic factors (Gindl et al., 2000; Cuny et al., 2015). Hence, the analysis of tree rings density can supplement the climatic information not captured by radial growth, by characterizing the overall count of radial growth cells, their radial dimensions, and the thickness of their cell walls (Wimmer and Grabner, 2000; Wu et al., 2005; Yuan et al., 2008). Methodological innovations, such as microdensity profiling via X-ray densitometry (Schneider et al., 2015) and blue-light intensity calibration (Campbell et al., 2007), now enable cellular-scale climate signal extraction. The demonstrated superiority of latewood density for temperature reconstruction in boreal systems (Fonti et al., 2010; Büntgen et al., 2021), coupled with density-carbon sequestration linkages (Camarero et al., 2021), positions dendroanatomical metrics as vital tools for assessing forest carbon sink trajectories. Despite these advances, ring-width indices remain disproportionately utilized in dendroclimatology (Zhang et al., 2011b; Duan et al., 2020), particularly in cold-humid regions where density parameters exhibit heightened thermal sensitivity (Bouriaud et al., 2005). This study addresses critical knowledge gaps in northeastern China's Greater Khingan Mountains (GKM) by employing Ps density chronologies to disentangle climate-forcing mechanisms and refine carbon sequestration models under anthropogenic warming.

GKM are the highest latitude region in China that is also quite sensitive to climate change (Ding and Dai, 1994; Wang et al., 1998; Xu, 1998). The connection between radial expansion of trees and climate in the GKM is now well understood (Zhang et al., 2016; Li et al., 2020). Specifically, the radial development of trees is primarily limited by regional hydrothermal conditions and varies with altitude (Bai et al., 2019; Wang et al., 2024b; Wang et al., 2024b), latitude (Jiang et al., 2016; Yasmeen et al., 2019), and slope direction (Liu and Liu, 2014). For example, as reported by Wang et al., older larch (*Larix decidua* Mill.) trees are more susceptible to summer temperature restrictions than middle-aged or young individuals (Wang et al., 2024a), and the climate sensitivity of Ps decreases with increasing altitude (Wang et al., 2024b). Despite these advances, the mechanistic drivers of density-climate interactions remain unresolved, particularly the hierarchical influence of specific climatic variables on Ps' lignification processes. This study targets the northwestern GKM foothills to: (1) develop high-resolution density chronologies through microdensitometric analysis, (2) quantify differential responses of density parameters (EWD, LWD, MXD, MND, TRD) to monthly/seasonal climatic variability, and (3) assess temporal stability of these relationships under accelerating warming. By elucidating unexplored dendroanatomical responses, our findings advance predictive models of boreal forest carbon dynamics and refine paleoclimatic reconstruction methodologies for thermally vulnerable high-latitude ecosystems.

2 Materials and methods

2.1 Study area

The GKM region is located in the northwest of Heilongjiang Province, which is part of the Eurasian Plate's high-latitude permafrost zone, situated at an altitude of 700–1,509 m a.s.l (Figure 1). This area is characterized by a distinctive cold temperate continental monsoon weather pattern. Affected by inland cold high pressure in winter, the climate is cold and dry, and affected by subtropical high warm air mass in summer, it is warm

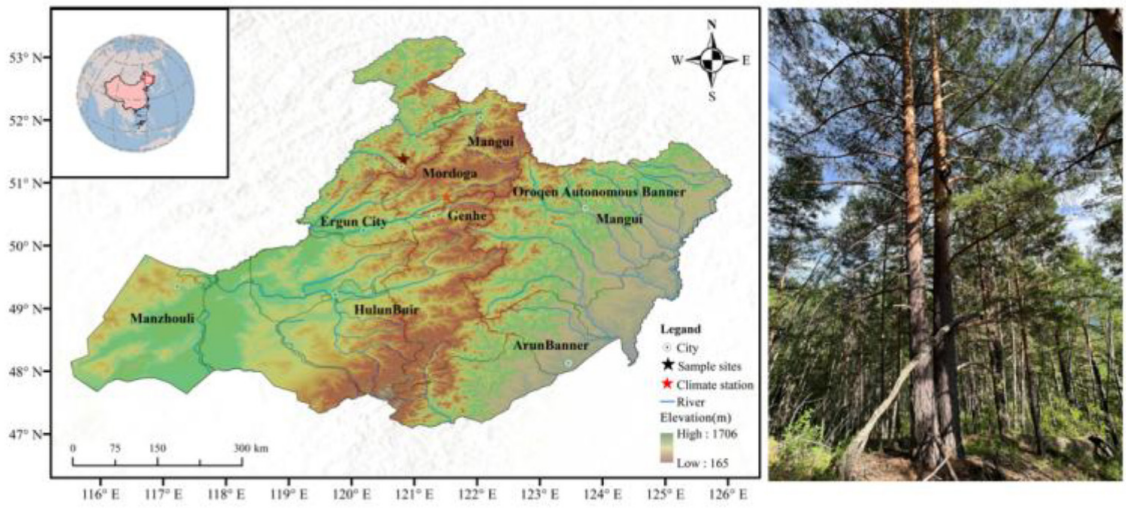

FIGURE 1
Map (left) showing the site where the tree rings were sampled of *Pinus sylvestris* var. *mongholica* (right).

and humid. The region has abundant rainfall, with an average annual precipitation of 460 mm, mainly concentrated in the rainy season (June to September), accounting for 74.8% of the annual precipitation. During the study period (1958–2020), the average annual temperature in the region was −4.1°C, the snow accumulation period lasted for 5 months, and the frost-free period lasted only 80–110 days. The soil type is mainly brown coniferous forest soil present in thin layers. The dominant tree species are larch (*Larix gmelinii* Mill.) and Ps. Other hardy tree species include *Betula platyphylla*, *Pinus pumila*, and *Picea koraiensis*. The tree species (Ps) selected for this study is the camphor pine, an Oriental variety of the European red pine that is widely distributed in the Eurasian temperate zone. It has a strong ability to withstand cold and drought, demonstrating high adaptability, being the most cold-tolerant species of the Chinese pines (*Pinus*).

2.2 Gathering samples and chronology establishment

The collection of samples from the primary forest area in the Moldoga region was completed at the end of July 2023, with minimal human impact. Using an increment borer, tree cores clearly unaffected by diseases, pests, fire, and other disturbances were collected at the diameter at breast height (1.3 m) of each Ps individual, with 2–3 cores taken from different directions per tree. This yielded a total of 53 cores taken from 24 trees (Table 1). Most of these sampled trees were dominant individuals over 100 years old.

The tree cores were transported to the lab, where they were dried, fixed, and polished. Their tree-ring widths were then measured using the German LINTAB6 ring width-measuring instrument (accurate to 0.001 mm) (Hart, 2011). After measuring the widths, the samples underwent routine processing for density data, which included desugaring, degreasing, segmenting, fixing, slicing, and the taking of X-ray films. The data of tree-ring wood density was obtained by Dendro2003 tree-ring density analysis system (Liu et al., 2021). Combined with these empirical tree-ring width measurements, COFECHA software was utilized to perform cross-dating tests on the measurement results (Holmes, 1983). The ARSTAN program's negative exponential function was applied to eliminate the tree growth trend. The double weight-averaging method was utilized to simulate the sequence into a normalized tree-ring density chronology (STD), a residual chronology (RES), and an autoregressive chronology (ARS) (Fritts, 1976). In comparing the statistical chronology of different chronology, we found that those of standard chronology often exceeded those of other chronology. So, we chose to focus on the correlative analysis of standard chronology and climate factors.

2.3 Climate data

Climate data from the nearest Genhe meteorological station (50°79′ N, 121°52′ E), for the period 1958 to 2020, were selected (Figure 2). Figure 2 illustrates the study area's monthly pattern of precipitation and temperature conditions for each year of that period. Based on the analysis of the trends in average annual temperature (T), maximum annual temperature (T_{max}), minimum annual temperature (T_{min}), and annual precipitation (P) at the Genhe meteorological station from 1958 to 2020 (Figure 3), it was found that the T, T_{max}, and T_{min} all showed a significant upward trend ($p < 0.001$), while the trend for P was not significant.

2.4 Data processing

We utilized SPSS 2022 software (Zhou et al., 2018) to compute the Pearson correlation coefficient between the tree-ring density chronology and each of the monthly climatic factors (T, T_{min}, T_{max}, P). In this study, only the standardized chronology with robust quality and highly correlated with climatic variables was

TABLE 1 Information on tree-ring core sampling.

Site code	Latitude (N)	Longitude (E)	Average altitude (m)	Slope direction	Slope (°)	Canopy density	Sample size
MHZ	51.35	120.86	1,100 (±20)	SE	30	0.7	24/53

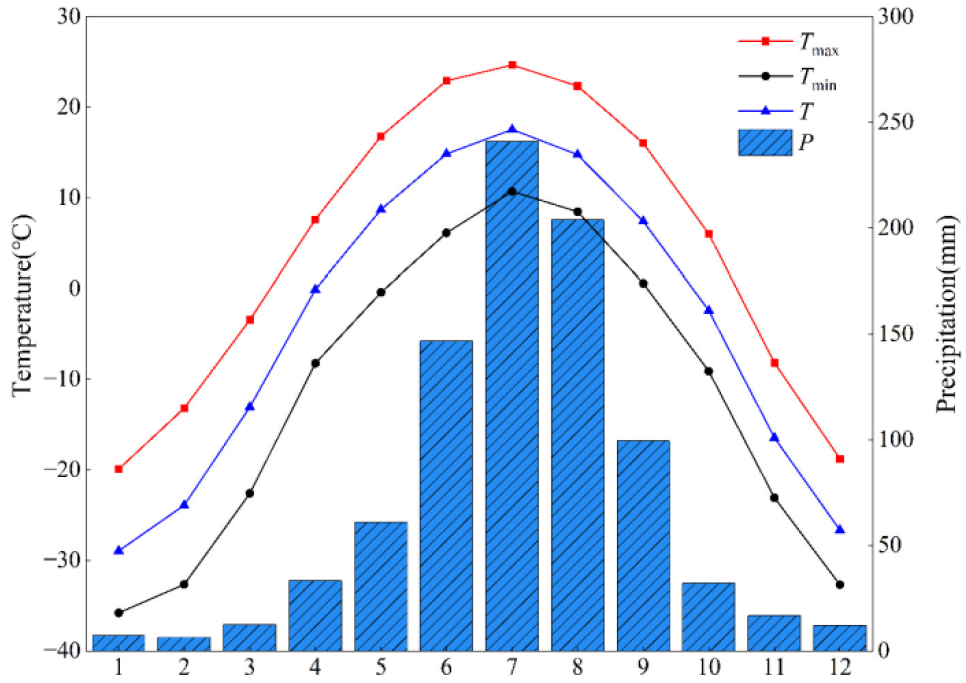

FIGURE 2
Mean monthly precipitation and temperature recorded at the Genhe meteorological station for 1958–2020.

utilized for the formal analysis. The formation of and change of tree rings are influenced by more than just the climatic factors of a single month, but also by the joint influence of climatic factors over several months (Sun et al., 2012). According to the ecophysiological significance of climate conditions for trees in the GKM, the growing season of Ps was divided into PAU (P9–P11) in autumn and WI (P12, C1–C2) in winter. SP (C3–C5) in spring, SU (C6–C8) in summer, and CAU (C9–C10) in autumn were used to study the relationship between tree-ring density and climatic variables, in different growth periods (Bao et al., 2019). To detect the relationships between tree growth and climatic variables, redundancy analysis (RDA) was used, this performed using CANOCO 5.0 software (Ter Braak and Smilauer, 2002), with density chronology designated as the dependent variable and the climatic factors as the explanatory variables. The forward-selection method was used to screen the climatic variables, one by one, and Monte Carlo permutation tests were conducted. These permutation tests were run 999 times, with the significance level established at $p < 0.05$. To test the stability of the relationship between Ps and climatic variables under the background of climate warming, moving correlation analysis between Ps and climatic variables was conducted from 1958 onward, using a 30-year sliding window size and a sliding window size of 1 year.

3 Results

3.1 Statistical characteristics of the density chronology of Ps

It can be seen from Table 2 that the MWC, SR, and EPS values of the TRD chronologies of Ps exceed those of other density chronologies. The results showed that for STD of the five different density indices of the Ps, the MMS values ranged from 0.040 to 0.053, reflecting the sensitivity of the chronology to climate information. This indicated that the changes in ring density of Ps trees in the GKM harbored substantial climate information, and the SR and overall representativeness of the samples were both high. The reliability of the ring density chronology is thus confirmed.

The MWC and SD between trees varied from 0.198 to 0.366 and from 0.225 to 0.267, respectively, suggesting that the ring width of the core samples was generally consistent, which could reflect the average growth of Ps. The FAC ranged from 0.809 to 0.896, suggesting that tree growth in the previous year had a certain impact on the current year's growth. The EPS of the sample ranged from 0.830 to 0.927, while the SR ranged from 4.898 to 12.660, indicating a high SR. This suggested that the created chronology had a high quality and was abundant in climate signals, confirming its suitability for dendroclimatology research.

TABLE 2 Statistical characteristics of the STD of tree-ring density of *Ps*.

Statistic characteristics	TRD	EWD	LWD	MXD	MND
Mean sensitivity (MS)	0.047	0.040	0.044	0.045	0.053
Standard deviation (SD)	0.225	0.277	0.227	0.231	0.267
First-order auto correlation (FAC)	0.877	0.895	0.896	0.885	0.809
Mean within-tree correlation (MWC)	0.366	0.317	0.299	0.297	0.198
Signal-to-noise ratio (SR)	12.660	9.613	9.620	9.554	4.898
Expressed population signal (EPS)	0.927	0.906	0.906	0.905	0.830
The first year of subsample signal strength > 0.85 (FSS)	1797	1797	1797	1797	1797
Sequence length (SL)	1694–2022	1694–2022	1694–2022	1694–2022	1694–2022

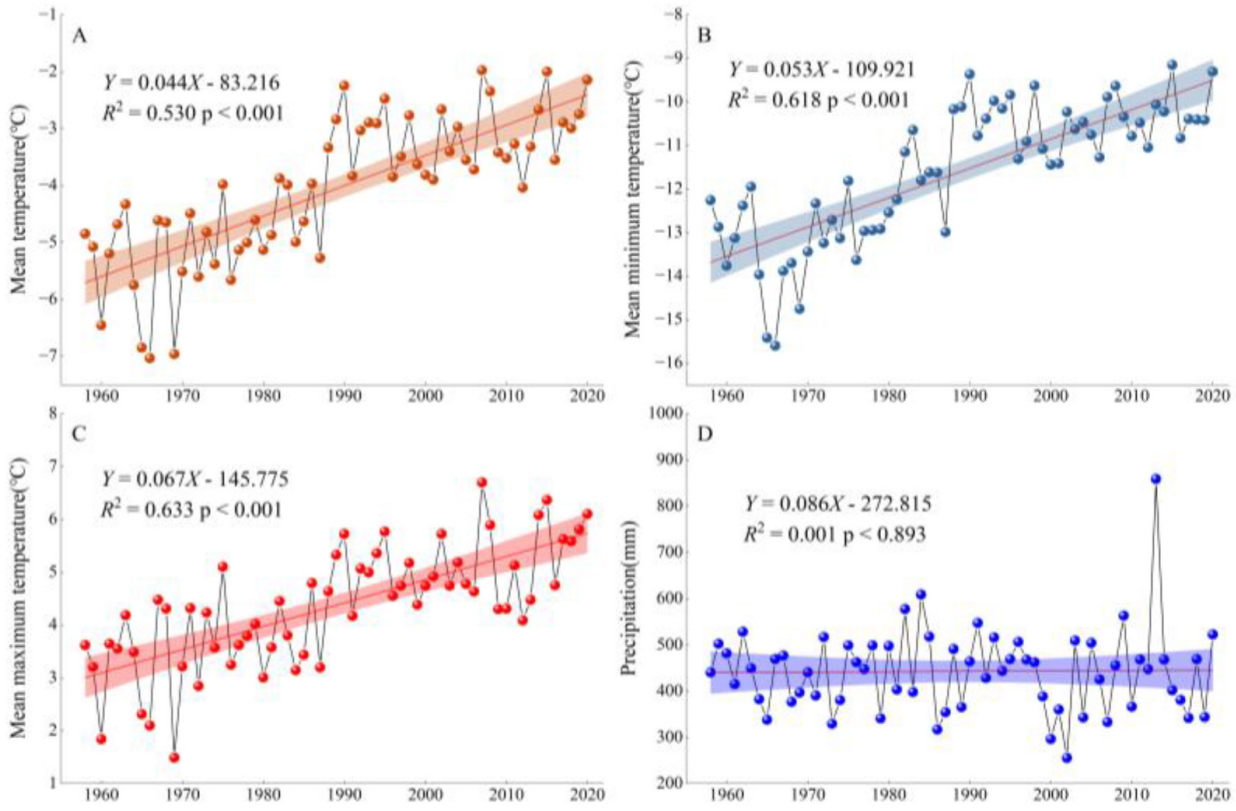

FIGURE 3
Linear trends in the climatic factors of the GKM from 1958 to 2020. **(A)** Mean temperature; **(B)** Mean minimum temperature; **(C)** Mean maximum temperature; **(D)** Precipitation.

The plotted sequence change curve of the five annual ring density STD (Figure 4) showed that their trends differed to some extent.

To describe the correlation of the density standardized chronology of Ps, the correlation values for all the density chronologies were calculated (Figure 5). These results revealed that TRW showed a positive effect with LWD and MXD, yet inversely related to EWD and MND, but not significantly correlated with TRD. However, TRD showed a positive effect with EWD, LWD, MXD, and EW ($p < 0.01$). Further, EWD showed a positive effect with LWD, MXD, and MND ($p < 0.01$), with the highest correlation coefficient attained with MND ($r = 0.91$, $p < 0.01$). Lastly, LWD showed a positive effect with MXD ($p < 0.01$).

3.2 Correlations between the density STD and climatic variables

The response analysis of STD chronologies to climatic variables (Figure 6) demonstrated that all density indices were temperature- and precipitation-sensitive, albeit with divergent seasonal drivers. Tracheidal radial diameter TRD and EWD both showed significant positive correlations ($p < 0.05$) with T_{max}. Unique to EWD were strong negative associations with October T and T_{max} from the preceding year, coupled with inverse relationships to May–July P. While latewood density LWD and MXD shared positive responses to March precipitation, MXD additionally correlated with October precipitation of the prior year. Notably, MND

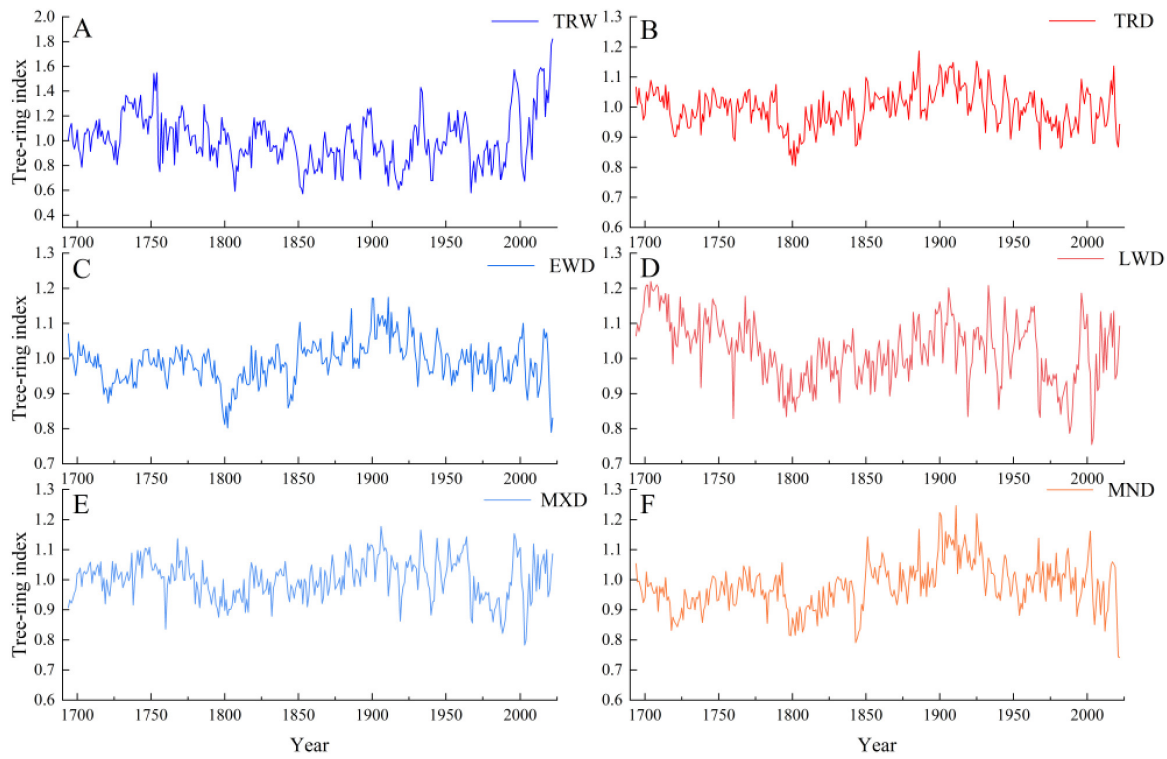

FIGURE 4
Change trend of tree-ring density Index of PS. **(A)** Tree-ring width index, TRW; **(B)** tree-ring density index, TRD; **(C)** minimum density, MND; **(D)** earlywood density, EWD; **(E)** maximum density, MXD; **(F)** latewood density, LWD.

exhibited pronounced negative correlations with temperatures from October to December of the previous year and negative correlations with May–July precipitation in the current year. Response patterns highlighted climatic sensitivity parallels between EWD and TRD, contrasting sharply with MND's delayed response to antecedent climatic conditions.

3.3 Response analysis of the density STD and climatic variables on a seasonal scale

Whereas TRD was inversely related with P in the summer (Figure 7), EWD was considerably inversely related with T in the previous autumn and P in the spring. In contrast, LWD was significantly inversely related with P in PAU and CAU. Likewise, MXD had a positive effect with P in PAU. However, MND was considerably inversely related not only with temperature in PAU and CAU, but also with precipitation in the spring and summer.

3.4 Redundancy analysis of the density STD and climatic variables of Ps

To further verify the connections between growth rings and climatic variables at the northwest foot of the GKM, redundancy analysis was conducted for the five density indices of Ps and the highly correlated climatic factors (Figure 8). There was a significant positive effect between MND and T_{max} in June, and a considerably inversely effect between MND and T and T_{min} in the autumn of the previous year. Moreover, MXD and LWD were had a considerably positive effect with P in October and March of the previous year. There was a considerably inversely correlation between EWD and T in the autumn of the previous year and P in the summer of the previous year. Finally, there was a considerably inversely effect between TRD and P in the summer.

3.5 Stability relationship between the density STD and climatic variables

To accurately reflect the temporal stability of growth of Ps trees in reaction to climate change, the 31-year sliding correlation values of tree-ring density chronology and four climatic variables were calculated for the 1958–2020 period. These results (Figure 9) uncovered a varying sensitivity level of the density STD to hydrothermal factors during 1958–2020, with correlation coefficients changing positively or negatively in different periods. Notably, TRD had a considerably positive effect with T and $T_{\max}$ in May of the same year and P in October of the previous year, yet inversely related with average precipitation in May of the same year, reaching significant levels in most of the time intervals assessed. For EWD and MND, each had a considerably positive effect with temperature in December of the previous year and P from May to July of the previous year. The correlation between LWD and MXD and $T_{\min}$ in May of the same year shifted from significantly negative to inverse.

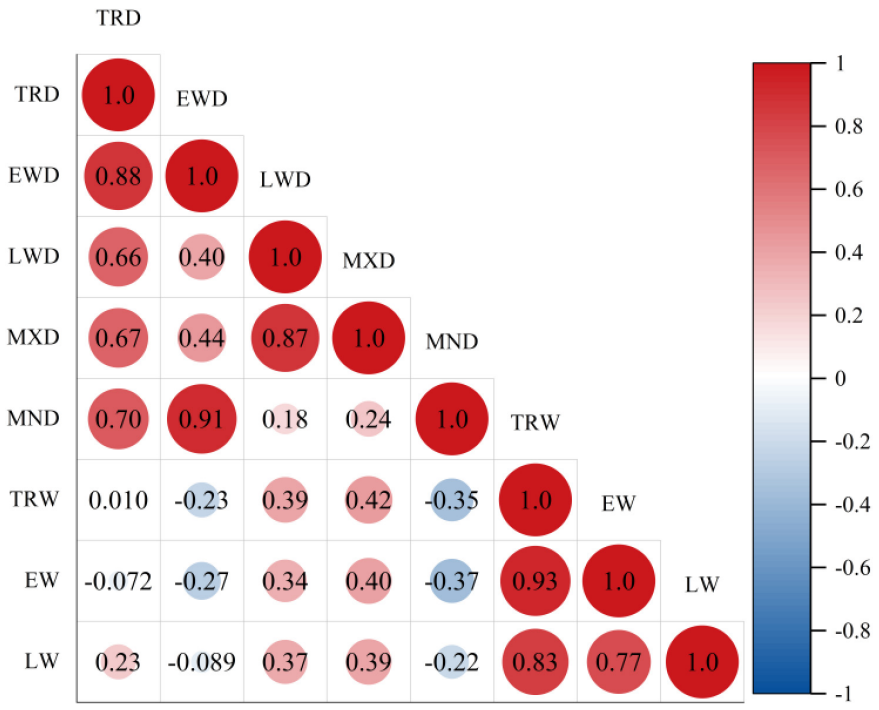

FIGURE 5
Correlation coefficients of tree growth ring indexes of Ps. Tree-ring width index (TRW), earlywood width index (EW), latewood width index (LW), tree-ring density index (TRD), minimum density (MND), earlywood density (EWD), maximum density (MXD), and latewood density (LWD).

4 Discussion

Previous studies across conifer species demonstrate that tree-ring density variations originate from cambial regulation of cell wall deposition versus lumen expansion during tracheid maturation (Silkin and Kirdyanov, 2003; Xu et al., 2011; Xu et al., 2013; Björklund et al., 2017). Our analysis of Ps rings advances this framework by linking cellular processes to climate-growth interactions: the negative correlations between TRW and EWD/MND emerge when favorable conditions drive accelerated radial growth, favoring tracheid expansion over secondary wall thickening—a carbon allocation trade-off analogous to that reported in Picea abies (Rathgeber, 2017). These dynamics reflect distinct cambial phases in Ps: earlywood forms large-diameter cells with extended expansion and limited wall thickening, whereas latewood development under cooler temperatures reduces cell division rates, truncates expansion duration, and prolongs wall-thickening periods, producing smaller cells with thicker walls (Cuny et al., 2014). Comparable patterns occur in *Larix mastersiana* (Li et al., 2024), *Cunninghamia lanceolata* (Zhang et al., 2021), and *Picea crassifolia* (Yang et al., 2012), underscoring conserved physiological strategies across montane conifers.

Redundancy analysis revealed significant climatic controls on ring density chronologies in the northwest foothills of the GKM, with EWD exhibiting strong positive correlations to June T_{max} and negative associations with May–July precipitation, consistent with European and Qilian Mountain dendroclimatic patterns (Wang et al., 2010). The April–June period—concurrent with earlywood formation and peak cambial activity—typically features sufficient soil moisture that decouples tree growth from water limitations (Zhang et al., 2021), establishing temperature as the primary driver of Ps radial growth, while precipitation exerts secondary influence (Yang et al., 2012). Elevated June T_{max} likely enhances earlywood development by extending the growth period and boosting carbon assimilation, thereby supporting structural maturation of both earlywood and latewood cells (Yang et al., 2012). Conversely, abundant growing-season precipitation promotes vigorous cell expansion through optimal hydration, yielding larger lumens with thinner walls that collectively reduce wood density (Liu and Ma, 1999; Camarero et al., 2017). TRD demonstrated positive sensitivity to May T_{max}, potentially through thermal acceleration of budburst and needle elongation that enhances carbohydrate production (Rossi et al., 2011; Hoeber et al., 2014), a process amplified by improved photosynthetic efficiency under adequate hydration and elevated transpiration rates (Jyske et al., 2010). However, supraoptimal summer temperatures may suppress metabolic enzymes and induce stomatal closure, ultimately constraining photosynthate allocation to cell wall deposition and EWD development (Martínez-Sancho et al., 2020).

The negative correlation between MND and prior-year October–December temperatures (Rossi et al., 2006) likely stems from delayed dormancy induced by elevated autumn temperatures, which reduces non-structural carbohydrate (NSC) reserves (Babst et al., 2019) and subsequently restricts cell wall thickening during earlywood formation in the following growing season. Similarly, the negative association between MND and current-year May–July precipitation reflects water-mediated prioritization of radial cell expansion over secondary wall lignification (Cuny et al., 2015), a carbon allocation trade-off widely observed in xylogenesis

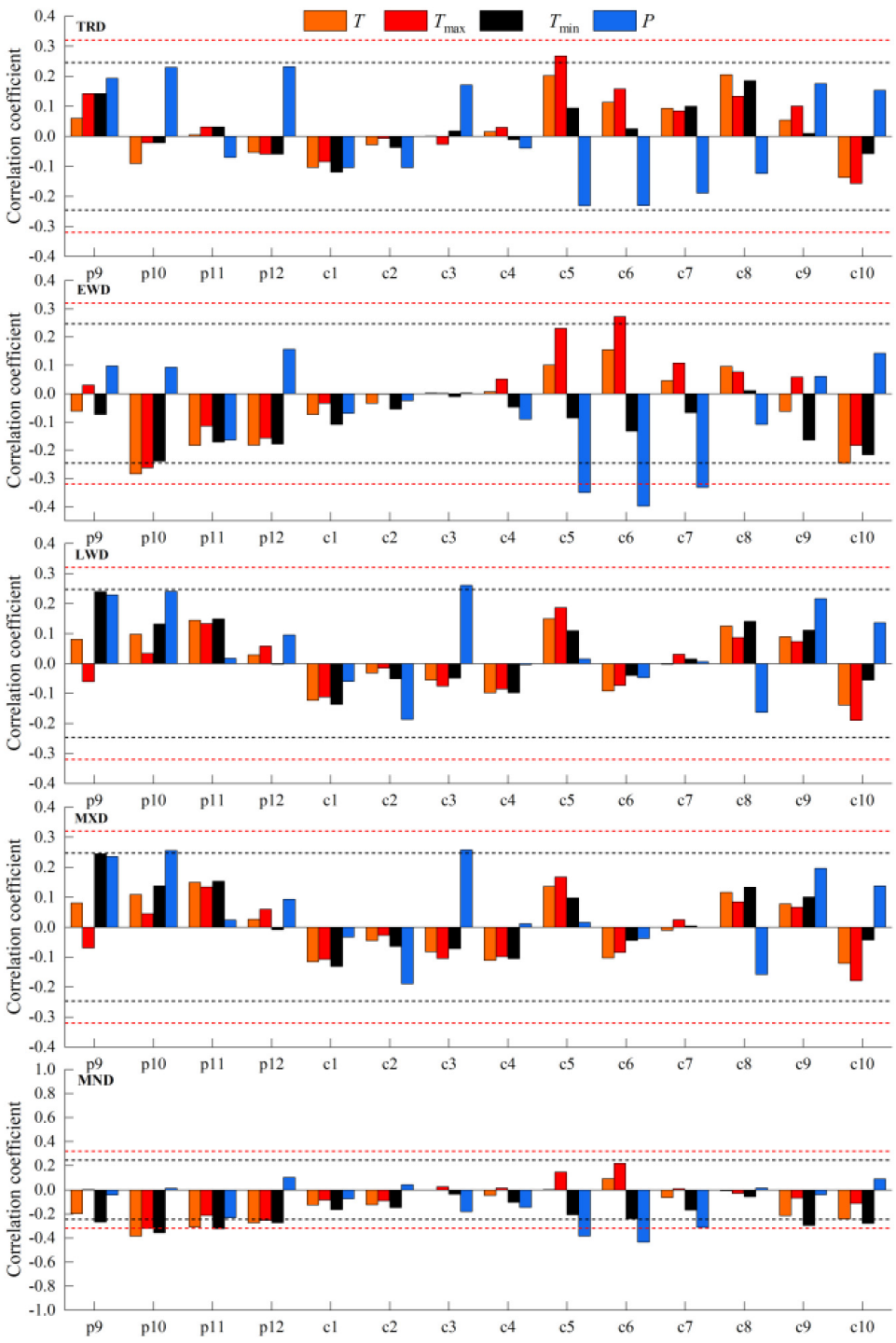

FIGURE 6
Correlation analysis of the density chronology and climatic variables of Ps. — (black dashed), $p < 0.05$, —(red dashed), $p < 0.01$. p, previous year; c, current year.

studies of temperate species (Fonti et al., 2010). Earlywood formation coinciding with growing season initiation (Atkin et al., 2007) creates dual thermal impacts: while rising temperatures stimulate metabolic activity and sap flux (Bai et al., 2016), excessive nocturnal warming exacerbates hydraulic stress through heightened soil evaporation and nocturnal transpiration (Zhang et al., 2011a), progressively depleting diurnal photosynthates essential for earlywood cell expansion. The significant positive relationships between May mean temperature and both MXD and LWD further confirm that optimal early-season thermal conditions promote latewood density development through extended cell wall thickening phases. These mechanistic interpretations align with redundancy analysis outcomes, reinforcing the robustness of response function results.

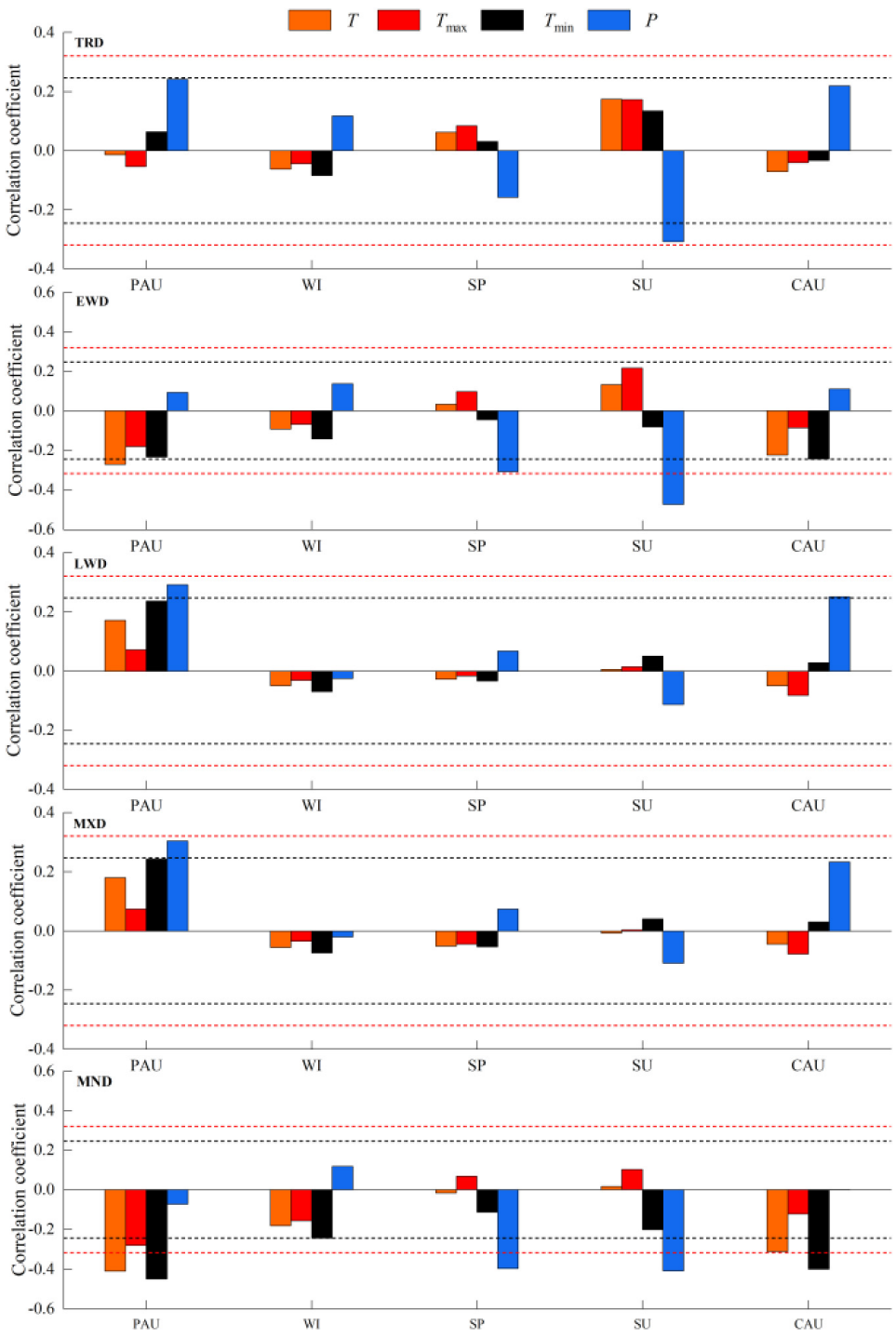

FIGURE 7
Correlation analysis of tree-ring density chronology and seasonal climatic factors of Ps.

Correlation analyses between density STD and climatic variables (Figures 3, 4) revealed predominant thermal control over interannual density variations in Ps, with MND demonstrating heightened sensitivity to T_{min}. Notably, MND exhibited inverse correlations with post-growing season temperatures (PAU), contrasting with the positive T_{min} associations observed in other seasons. Autumnal thermal elevation prolongs cambial activity, enhancing carbohydrate reserves for subsequent growth while accelerating next-year's radial expansion (Gou et al., 2008; Zhang et al., 2013; Zhang T. et al., 2020). Conversely, suboptimal autumn temperatures (particularly October minima) reduce bud dormancy establishment, impairing subsequent growing-season productivity (Wang et al., 2011). Concurrent late-season warmth and precipitation deficits amplify plant respiration and evapotranspiration, inducing soil moisture depletion and elevated vapor pressure deficits that constrain radial

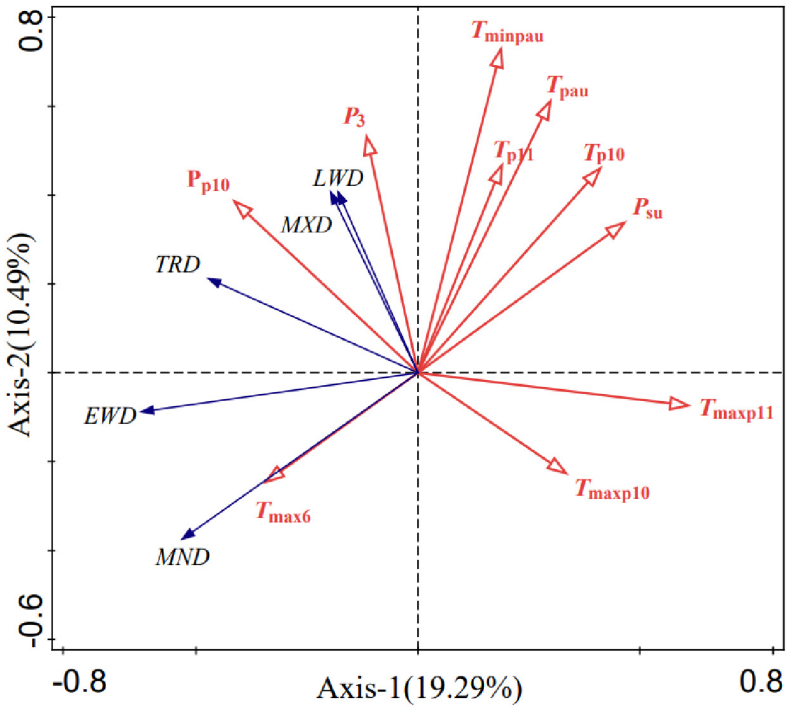

FIGURE 8
Redundancy analysis of climatic variables and the density STD of Ps.

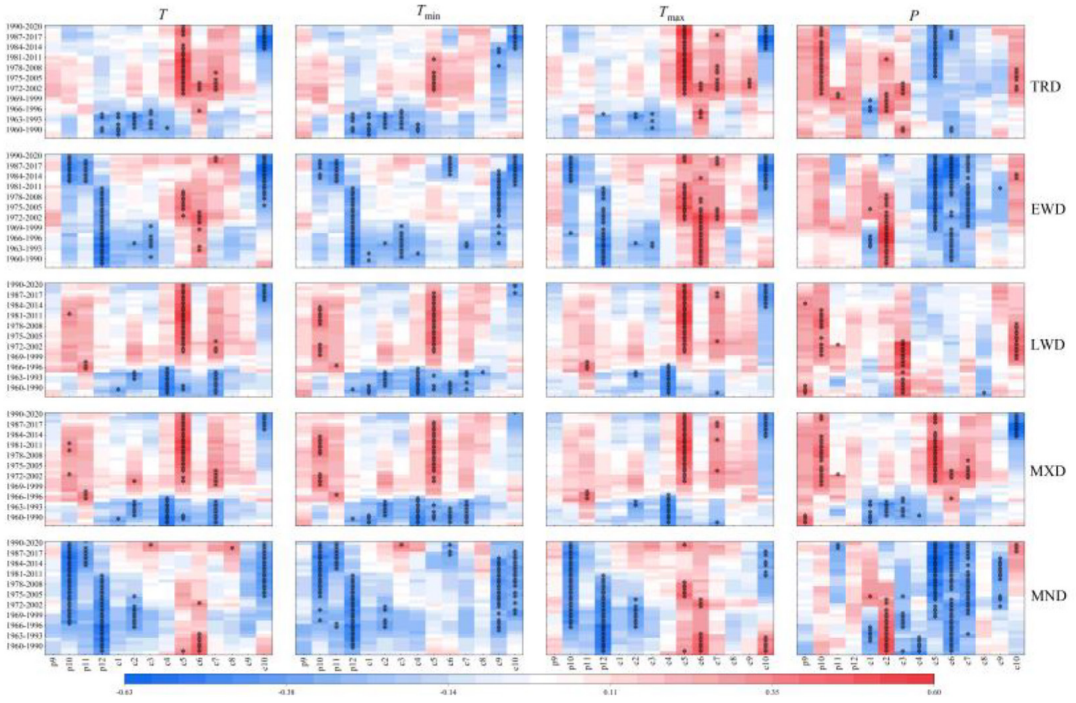

FIGURE 9
Correlation analysis between the density STD and seasonal climatic variables of Ps.

expansion while promoting density through impaired nutrient translocation (Yu et al., 2021). The lagged climatic sensitivity of MND mirrors findings in *Picea mariana* populations from northwestern Canada (Xiang et al., 2019), indicating carryover effects of prior-year physiological processes on current growth trajectories.

EWD and MND showed inverse correlations with spring-summer precipitation, whereas LWD and MXD displayed positive

associations with prior autumn precipitation. During peak cambial activity in spring and summer, abundant precipitation alleviates hydraulic constraints, facilitating rapid tracheid expansion that prioritizes lumen enlargement over wall thickening-a mechanism explaining reduced EWD and MND under high rainfall regimes (Liu and Ma, 1999; Kharuk et al., 2019). Conversely, autumn precipitation enhances lignification processes through prolonged carbohydrate availability, enabling sustained secondary wall deposition that elevates subsequent-year LWD and MXD. The absence of significant LWD/MXD correlations with summer rainfall likely reflects non-limiting soil moisture conditions during early growing seasons, as rising temperatures coupled with high humidity and soil water saturation negate precipitation's role as a growth-limiting factor for Ps.

Our analysis identified temporal instability in climate-density relationships across the five anatomical density indices, reflecting both discrete climatic signals encoded in different wood anatomical features and divergent response thresholds to environmental drivers. The marked warming trend observed in the GKM region has substantially modulated density-climate couplings, particularly through thermal impacts on carbon allocation dynamics. TRD exhibited positive correlations with May T and T_{max}, while LWD and MXD showed transitional sensitivity to May T_{min}-shifting from historically negative to recent positive associations that persisted across multiple temporal scales. This polarity reversal likely stems from warming-induced diurnal thermal asymmetry: elevated daytime temperatures enhance photosynthetic carbon assimilation, offsetting nocturnal respiratory carbon efflux exacerbated by Tmin increases, thereby sustaining net carbon gain for structural growth (Gou et al., 2007; Zhu and Zheng, 2022). Concurrently, Ps may exhibit autonomous physiological adjustments under evolving summer thermal and hydric optima (Zhang H. et al., 2020). Notably, EWD and MND maintained inverse correlations with prior-year December temperatures and antecedent May–July precipitation, potentially linked to climate-driven enhancements in hydraulic efficiency and pre-season cambial reactivation (Cerrato et al., 2019).

Climatic fluctuations exert dual influences on forest ecosystems, directly modulating physiological processes (growth rates, bud phenology, reproductive cycles) while indirectly restructuring stand dynamics through altered disturbance regimes (Loehle and Leblanc, 1996). Progressive warming—particularly diurnal thermal asymmetry—is reshaping the ecophysiological thresholds of Ps and boreal conifers, potentially inducing divergence in traditional density-climate relationships through "growth-decoupling" mechanisms (Olivar et al., 2015; Su et al., 2023). This phenomenon aligns with documented "divergence problems" in high-latitude Northern Hemisphere forests, where warming-induced physiological stressors disrupt historical growth-climate couplings (D'Arrigo et al., 1992). Current research disproportionately focuses on radial growth responses, leaving critical knowledge gaps regarding density parameter stability under shifting climate forcings-an urgent priority for dendroanatomical studies. Our findings demonstrate enhanced sensitivity of density chronologies to early-growing-season T_{min} variability, revealing their superior capacity for resolving fine-scale thermal histories compared to traditional ring-width proxies, thus positioning wood density as a critical tool for paleoclimatic reconstruction in thermally volatile boreal regions.

5 Conclusion

This study elucidates the climate regulation mechanism of tree ring density parameters in the GKM, and reveals their differential sensitivity to seasonal hydrothermal driving factors. The EWD was positively correlated with the starting temperature of the growth period and negatively correlated with the thermal and hydrological conditions before autumn, reflecting the regulating effect of interannual carbohydrate transport dynamics. MND was negatively correlated with the previous year's winter temperature and the current growing season precipitation, highlighting its role as a carbon partition tradeoff indicator during cell wall thickening. Time analysis shows that the climate response is non-stationary: Post-1980s climate change triggered a polarity reversal of MXD sensitivity to the May minimum temperature and amplified the coupling of LWD with spring precipitation, suggesting regulation of photocopier-respiratory balance under asymmetric daily warming. Cambium phenology controls these reactions–early wood formation depends on temperature-mediated cell expansion timing, while the lignification phase of late wood takes precedence over water-confined wall deposition. Gradual warming disrupts these stage-specific processes through nighttime breathing surges and fall hydraulic restrictions, fundamentally reshaping the coordination between tracheid enlargement and secondary wall development. These findings establish a critical threshold for density-climate coupling and advance the understanding of the mechanisms by which boreal conifers adapt to changes in hydrothermal state.

Data availability statement

The raw data supporting the conclusions of this article will be made available by the authors, without undue reservation.

Author contributions

XW: Formal Analysis, Investigation, Methodology, Writing – original draft. ZW: Formal Analysis, Validation, Visualization, Writing – original draft. DZ: Data curation, Funding acquisition, Project administration, Writing – review and editing. SY: Funding acquisition, Methodology, Project administration, Resources, Supervision, Writing – review and editing. TZ: Project administration, Resources, Supervision, Writing – review and editing. TL: Formal Analysis, Investigation, Methodology, Software, Visualization, Writing – original draft. XL: Data curation, Formal Analysis, Methodology, Software, Visualization, Writing – original draft. BD: Data curation, Formal Analysis, Methodology, Writing – original draft. XC: Methodology, Software, Validation, Visualization, Writing – original draft.

Funding

The authors declare that financial support was received for the research and/or publication of this article. This research

was funded by the National Natural Science Foundation of China (No.41671064) and the Natural Science Foundation of Heilongjiang Province (No. LH 2021D012).

Acknowledgments

We would like to thank the authors for their assistance with the manuscript.

Conflict of interest

The authors declare that the research was conducted in the absence of any commercial or financial relationships that could be construed as a potential conflict of interest.

Generative AI statement

The authors declare that no Generative AI was used in the creation of this manuscript.

Publisher's note

All claims expressed in this article are solely those of the authors and do not necessarily represent those of their affiliated organizations, or those of the publisher, the editors and the reviewers. Any product that may be evaluated in this article, or claim that may be made by its manufacturer, is not guaranteed or endorsed by the publisher.

References

Anderegg, W. R., Wu, C., Acil, N., Carvalhais, N., Pugh, T. A., Sadler, J. P., et al. (2022). A climate risk analysis of Earth's forests in the 21st century. *Science* 377, 1099–1103. doi: 10.1126/science.abp9723

Atkin, O., Scheurwater, I., and Pons, T. (2007). Respiration as a percentage of daily photosynthesis in whole plants is homeostatic at moderate, but not high, growth temperatures. *New Phytol.* 174, 367–380. doi: 10.1111/j.1469-8137.2007.02011.x

Babst, F., Bouriaud, O., Poulter, B., Trouet, V., Girardin, M. P., and Frank, D. C. (2019). Twentieth century redistribution in climatic drivers of global tree growth. *Sci. Adv.* 5:eaat4313. doi: 10.1126/sciadv.aat4313

Bai, X., Zhang, X., Li, J., Duan, X., Jin, Y., and Chen, Z. (2019). Altitudinal disparity in growth of Dahurian larch (*Larix gmelinii* Rupr.) in response to recent climate change in northeast China. *Sci. Total Environ.* 670, 466–477. doi: 10.1016/j.scitotenv.2019.03.232

Bai, Z., Liu, H., Yu, C., Liu, D., and Han, Y. (2016). Dynamic changes of sap flow in the trunk of *Larix sibirica* Ledeb. *J. Agric. Univer. Hebei* 39, 49–54.

Bao, A., Yang, L., and Liu, B. (2019). Radial growth of *Pinus koraiensis* and *Juglans mandshurica* in response to climate change in Laoyeling mountains. *J. Northeast Forestry Univer.* 47, 16–21. doi: 10.3389/ffgc.2024.1343730

Björklund, J., Seftigen, K., Schweingruber, F., Fonti, P., Von Arx, G., Bryukhanova, M. V., et al. (2017). Cell size and wall dimensions drive distinct variability of earlywood and latewood density in Northern Hemisphere conifers. *New Phytol.* 216, 728–740. doi: 10.1111/nph.14639

Bouriaud, O., Leban, J.-M., Bert, D., and Deleuze, C. (2005). Intra-annual variations in climate influence growth and wood density of Norway Spruce. *Tree Physiol.* 25, 651–660. doi: 10.1093/treephys/25.6.651

Büntgen, U., Urban, O., Krusic, P. J., Rybníček, M., Kolář, T., Kyncl, T., et al. (2021). Recent European drought extremes beyond Common Era background variability. *Nat. Geosci.* 14, 190–196. doi: 10.1038/s41561-021-00698-0

Camarero, J. J., and Gutiérrez, E. (2017). Wood density of silver fir reflects drought and cold stress across climatic and biogeographic gradients. *Dendrochronologia* 45, 101–112. doi: 10.1016/j.dendro.2017.07.005

Camarero, J. J., Fernández-Pérez, L., Kirdyanov, A. V., Shestakova, T. A., Knorre, A. A., Kukarskih, V. V., et al. (2017). Minimum wood density of conifers portrays changes in early season precipitation at dry and cold Eurasian regions. *Trees* 31, 1423–1437. doi: 10.1007/s00468-017-1559-x

Camarero, J. J., Gazol, A., Sangüesa-Barreda, G., Vergarechea, M., Alfaro-Sánchez, R., Cattaneo, N., et al. (2021). Tree growth is more limited by drought in rear-edge forests most of the times. *Forest Ecosyst.* 8, 1–15. doi: 10.1186/s40663-021-00303-1

Campbell, R., Mccarroll, D., Loader, N. J., Grudd, H., Robertson, I., and Jalkanen, R. (2007). Blue intensity in Pinus sylvestris tree-rings: Developing a new palaeoclimate proxy. *Holocene* 17, 821–828. doi: 10.1177/0959683607080523

Cerrato, R., Salvatore, M. C., Gunnarson, B. E., Linderholm, H. W., Carturan, L., Brunetti, M., et al. (2019). A *Pinus cembra* L. tree-ring record for late spring to late summer temperature in the Rhaetian Alps. *Italy. Dendrochronologia* 53, 22–31. doi: 10.1016/j.dendro.2018.10.010

Chen, L., Huang, J.-G., Stadt, K. J., Comeau, P. G., Zhai, L., Dawson, A., et al. (2017). Drought explains variation in the radial growth of white spruce in western Canada. *Agric. For. Meteorol.* 233, 133–142. doi: 10.1016/j.agrformet.2016.11.012

Cuny, H. E., Rathgeber, C. B., Frank, D., Fonti, P., and Fournier, M. (2014). Kinetics of tracheid development explain conifer tree-ring structure. *New Phytol.* 203, 1231–1241. doi: 10.1111/nph.12871

Cuny, H. E., Rathgeber, C. B., Frank, D., Fonti, P., Mäkinen, H., Prislan, P., et al. (2015). Woody biomass production lags stem-girth increase by over one month in coniferous forests. *Nat. Plants* 1, 1–6. doi: 10.1038/nplants.2015.160

D'Arrigo, R. D., Jacoby, G. C., and Free, R. M. (1992). Tree-ring width and maximum latewood density at the North American tree line: Parameters of climatic change. *Can. J. Forest Res.* 22, 1290–1296. doi: 10.1139/x92-171

Ding, Y., and Dai, X. (1994). Temperature variation in China during the last 100 years. *Meteorology* 20, 19–26.

Duan, J., Li, L., Ma, Z., and Chen, L. (2020). Post-industrial late summer warming recorded in tree-ring density in the eastern Tibetan Plateau. *Int. J. Climatol.* 40, 795–804. doi: 10.1002/joc.6239

Esper, J., Klippel, L., Krusic, P. J., Konter, O., Raible, C. C., Xoplaki, E., et al. (2020). Eastern Mediterranean summer temperatures since 730 CE from Mt. Smolikas tree-ring densities. *Clim. Dyn.* 54, 1367–1382. doi: 10.1007/s00382-019-05063-x

Fonti, P., Von Arx, G., García-González, I., Eilmann, B., Sass-Klaassen, U., Gärtner, H., et al. (2010). Studying global change through investigation of the plastic responses of xylem anatomy in tree rings. *New Phytol.* 185, 42–53. doi: 10.1111/j.1469-8137.2009.03030.x

Fritts, H. (1976). *Tree Rings and Climate*. New York: Academic Press.

Fritts, H. (1991). *Reconstruction Large Scale Climate Patterns From Tree-Ring Data, Tuson, USA*. Arizona: The Arizona University Press.

Gindl, W., Grabner, M., and Wimmer, R. (2000). The influence of temperature on latewood lignin content in treeline Norway Spruce compared with maximum density and ring width. *Trees* 14, 409–414. doi: 10.1007/s004680000057

Gou, X., Chen, F., Yang, M., Gordon, J., Fang, K., Tian, Q., et al. (2008). Asymmetric variability between maximum and minimum temperatures in Northeastern Tibetan Plateau: Evidence from tree rings. *Sci. China Series D Earth Sci.* 51, 41–55. doi: 10.1007/s11430-007-0154-1

Gou, X., Chen, F., Yang, M., Jacoby, G., Fang, K., Tian, Q., et al. (2007). *Asymmetric Changes in Maximum and Minimum Temperatures Revealed by Tree-Ring Records in the Northeastern Tibetan Plateau*. Beijing: Science China Press, 1480–1492.

Hart, S. J. (2011). *Fundamentals of Tree-Ring Research*. Tucson, AZ: University of Arizona Press. doi: 10.1080/00330124.2010.536466

Hoeber, S., Leuschner, C., Köhler, L., Arias-Aguilar, D., and Schuldt, B. (2014). The importance of hydraulic conductivity and wood density to growth performance in eight tree species from a tropical semi-dry climate. *Forest Ecol. Manag.* 330, 126–136. doi: 10.1016/j.foreco.2014.06.039

Holmes, R. L. (1983). Computer-assisted quality control in tree-ring dating and measurement. *Tree-Ring Bull.* 43, 69–78. doi: 10.1016/j.dib.2018.08.019

Jiang, Y., Zhang, J., Han, S., Chen, Z., Setälä, H., Yu, J., et al. (2016). Radial growth response of Larix gmelinii to climate along a latitudinal gradient in the Greater Khingan Mountains. *Northeastern China. Forests* 7:295. doi: 10.3390/f7120295

Jyske, T., Hölttä, T., Mäkinen, H., Nöjd, P., Lumme, I., and Spiecker, H. (2010). The effect of artificially induced drought on radial increment and wood properties of Norway spruce. *Tree Physiol.* 30, 103–115. doi: 10.1093/treephys/tpp099

Kharuk, V. I., Ranson, K. J., Petrov, I. Y. A., Dvinskaya, M. L., Im, S. T., and Golyukov, A. S. (2019). Larch (Larix dahurica Turcz) growth response to climate change in the Siberian permafrost zone. *Regional Environ. Change* 19, 233–243. doi: 10.1007/s10113-018-1401-z

Kikstra, J. S., Nicholls, Z. R., Smith, C. J., Lewis, J., Lamboll, R. D., Byers, E., et al. (2022). The IPCC Sixth Assessment Report WGIII climate assessment of mitigation pathways: From emissions to global temperatures. *Geosci. Model Dev.* 15, 9075–9109. doi: 10.5194/gmd-15-9075-2022

Li, M., Duan, J., and Wang, L. (2024). Differences in responses of tree-ring width and density of Larix mastersiana to climatic factors in the west Sichuan Platea. *Quaternary Res.* 44, 963–975.

Li, W., Jiang, Y., Dong, M., Du, E., Zhou, Z., Zhao, S., et al. (2020). Diverse responses of radial growth to climate across the southern part of the Asian boreal forests in northeast China. *For. Ecol. Manag.* 458:117759. doi: 10.1016/j.foreco.2019.117759

Liang, R., Sun, Y., Qiu, S., Wang, B., and Xie, Y. (2023). Relative effects of climate, stand environment and tree characteristics on annual tree growth in subtropical Cunninghamia lanceolata forests. *AgriculturalForest Meteorol.* 342:109711. doi: 10.1016/j.agrformet.2023.109711

Liu, K., Zhang, T., Zhang, R., Yu, S., Huang, L., Jiang, et al. (2021). Characteristics of tree-ring density at different stem heights and their climatic responses. *Chin. J. Appl. Ecol.* 32, 503–512. doi: 10.13287/j.1001-9332.202102.027

Liu, X., and Liu, B. (2014). Response of Larix gmelinii (Rupr.) Kuzen radial growth to climate for different slope direction in daxing'an mountain. *J. Northeast For. Univer.* 42, 13–21.

Liu, Y., and Ma, L. (1999). Seasonal precipitation reconstruction from tree ring widths for the last 376 years in Hohhot region. *Chin. Sci. Bull.* 44, 1986–1991.

Loehle, C., and Leblanc, D. (1996). Model-based assessments of climate change effects on forests: A critical review. *Ecol. Modell.* 90, 1–31. doi: 10.1016/0304-3800(96)83709-4

Martínez-Sancho, E., Slámová, L., Morganti, S., Grefen, C., Carvalho, B., Dauphin, B., et al. (2020). The GenTree Dendroecological Collection, tree-ring and wood density data from seven tree species across Europe. *Sci. Data* 7:1. doi: 10.1038/s41597-019-0340-y

Olivar, J., Rathgeber, C., and Bravo, F. (2015). Climate change, tree-ring width and wood density of pines in Mediterranean environments. *Iawa Journal* 36, 257–269. doi: 10.1016/j.scitotenv.2022.159291

Rathgeber, C. B. (2017). Conifer tree-ring density interannual variability–anatomical, physiological and environmental determinants. *New Phytol.* 216, 621–625. doi: 10.1111/nph.14763

Rossi, S., Deslauriers, A., Anfodillo, T., Morin, H., Saracino, A., Motta, R., et al. (2006). Conifers in cold environments synchronize maximum growth rate of tree-ring formation with day length. *New Phytol.* 170, 301–310. doi: 10.1111/j.1469-8137.2006.01660.x

Rossi, S., Morin, H., Deslauriers, A., and Plourde, P.-Y. (2011). Predicting xylem phenology in black spruce under climate warming. *Glob. Change Biol.* 17, 614–625. doi: 10.1093/treephys/tpy151

Schneider, L., Smerdon, J. E., Büntgen, U., Wilson, R. J., Myglan, V. S., Kirdyanov, A. V., et al. (2015). Revising midlatitude summer temperatures back to AD 600 based on a wood density network. *Geophys. Res. Lett.* 42, 4556–4562. doi: 10.1002/2015GL063956

Silkin, P., and Kirdyanov, A. (2003). The relationship between variability of cell wall mass of earlywood and latewood tracheids in larch tree-rings, the rate of tree-ring growth and climatic changes. *Holzforschung* 57, 1–7. doi: 10.1515/HF.2003.001

Singh, V. P., Singh, R., Paul, P. K., Bisht, D. S., and Gaur, S. (2024). "Climate change impact analysis," in *Hydrological Processes Modelling and Data Analysis: A Primer*, eds V. P. Singh, R. Berndtsson, L. N. Rodrigues, et al. (Berlin: Springer), 105–126. doi: 10.1007/978-981-97-1316-5_5

Smerdon, J. E., Kaufman, D. S., Asrat, A., Kiefer, T., and Sigl, M. (2013). Continental-scale temperature variability during the past two millennia. *Nat. Geosci.* 6, 339–346. doi: 10.1038/ngeo1797

Su, R., Guo, E., Wang, Y., Yin, S., Gu, X., Kang, Y., et al. (2023). Extreme climate changes in the Inner Mongolia and their impacts on vegetation dynamics during 1982—2020. *Acta Ecol. Sin.* 43, 419–431. doi: 10.5846/stxb202112073469

Sun, Y., Wang, L., and Chen, J. (2012). Response of tree growth to climate change and reconstruction of summer temperature based on Korean larch. *J. Earth Environ.* 3, 889–899.

Ter Braak, C. J., and Smilauer, P. (2002). *"CANOCO Reference Manual and CanoDraw for Windows user's Guide: Software for Canonical Community Ordination (version 4.5)". www. canoco. com).*

Van Mantgem, P. J., Stephenson, N. L., Byrne, J. C., Daniels, L. D., Franklin, J. F., Fulé, P. Z., et al. (2009). Widespread increase of tree mortality rates in the western United States. *Science* 323, 521–524. doi: 10.1126/science.1165000

Wang, L., Duan, J., Chen, J., Huang, L., and Shao, X. (2010). Temperature reconstruction from tree-ring maximum density of Balfour spruce in eastern Tibet, China. *Int. J. Climatol.* 30, 972–979. doi: 10.1002/joc.2000

Wang, S., Ye, J., Gong, D., Zhu, J., and Yao, T. (1998). Construction of mean annual temperature series for the last one hundred years in China. *Quart. J. Appl. Meteorol.* 9, 392–401.

Wang, T., Li, C., Zhang, H., Ren, S., Li, L., Pan, N., et al. (2016). Response of conifer trees radial growth to climate change in Baotianman National Nature Reserve,central China. *Acta Ecol. Sin.* 36, 5324–5332. doi: 10.5846/stxb201501260209

Wang, X., Song, L., and Zhang, Y. (2011). Climate-tree growth relationships of *Pinus sylvestris* var. *mongolica* in the northern Daxing'an Mountains. *China. Chin. J. Plant Ecol.* 35, 294–302. doi: 10.3724/SP.J.1258.2011.00294

Wang, Z., Lyu, Y., Wang, W., Guo, X., and Dong, L. (2024a). Individual diameter growth of natural *Larix gmelinii* forests with different ages and their responses to climate change. *For. Eng.* 40, 39–48.

Wang, Z., Zhang, T., Zhang, D., Luo, T., Wang, X., Li, X., et al. (2024b). Responses of *Pinus sylvestris* var. *mongolica* tree ring width to climate factors at different elevations in the northern Greater Khingan Mountains. *Dendrochronologia* 83:126166. doi: 10.1016/j.dendro.2024.126166

Wimmer, R., and Grabner, M. (2000). A comparison of tree-ring features in Picea abies as correlated with climate. *IAWA J.* 21, 403–416. doi: 10.3389/fpls.2016.01602

Wu, P., Wang, L., and Shao, X. (2005). Reconstruction of summer temperature from maximum latewood density of Pinus densata in west sichuan. *Acta Geograph. Sin.* 06, 120–128.

Xiang, W., Hassegawa, M., Franceschini, T., Leitch, M., and Achim, A. (2019). Characterizing wood density–climate relationships along the stem in black spruce (*Picea mariana* (Mill.) *BSP*) using a combination of boosted regression trees and mixed-effects models. *For. Int. J. For. Res.* 92, 357–374. doi: 10.1093/forestry/cpz006

Xu, H. (1998). *China Daxinganling Forest*. Beijing: Science Press.

Xu, J., Lu, J., Bao, F., Evans, R., and Downes, G. M. (2013). Climate response of cell characteristics in tree rings of Picea crassifolia. *Holzforschung* 67, 217–225. doi: 10.1515/hf-2011-0144

Xu, J., Lv, J., Bao, F., Huang, R., Liu, X., Robert, E., et al. (2011). Response of wood density of *Picea crassifolia* to climate change in Qilian Mountains of northwestern China. *J. Beijing For. Univer.* 33, 115–121.

Yang, B., He, M., Shishov, V., Tychkov, I., Vaganov, E., Rossi, S., et al. (2017). New perspective on spring vegetation phenology and global climate change based on Tibetan Plateau tree-ring data. *Proc. Natl. Acad. Sci.* 114, 6966–6971. doi: 10.1073/pnas.1616608114

Yang, Y., Huang, Q., Liu, Y., Wang, Y., Bai, T., and Wang, W. (2012). Response analysis between climate factors and the density of wood growth of picea crassifolia. *Journal Xi'an Univer. Technol.* 28, 432–438.

Yasmeen, S., Wang, X., Zhao, H., Zhu, L., Yuan, D., Li, Z., et al. (2019). Contrasting climate-growth relationship between Larix gmelinii and Pinus sylvestris var. mongolica along a latitudinal gradient in Daxing'an Mountains, China. *Dendrochronologia* 58:125645. doi: 10.1016/j.dendro.2019.125645

Yu, J., Chen, J., Meng, S., Zhou, H., Zhou, G., Gao, L., et al. (2021). Response of radial growth of Pinus sylvestriformis and Picea jezoensis to climate warming in the ecotone of Changbai Mountain,Northeast China. *Chin. J. Appl. Ecol.* 32, 46–56. doi: 10.13287/j.1001-9332.202101.004

Yuan, Y., Jan, E., Wei, W., Danie, N., Anne, V., Yu, S., et al. (2008). Development and correlation of the maximum treering density of tree rings in three spruce trees in the western Tianshan Mountains of Xinjiang, and its correlation and climatic signal analysis. *Arid Land Geogr.* 31, 560–566.

Zhang, H., Yan, Y., Hu, Y., Huang, Z., Wu, P., and Ma, X. (2020). Analysis on the relationship between radial growth of Cunninghamia lanceolata and climatic factors based on tree-ring climate correlation. *J. Fujian Agric. For. Univer.* 49, 59–66.

Zhang, H., Zhang, Y., Hu, Y., Yan, Y., Wu, P., Zeng, A., et al. (2021). Response of tree ring density to climatic factors of Cunninghamia lanceolata under climate warming. *Acta Ecol. Sin.* 41, 1551–1563. doi: 10.5846/stxb201908261764

Zhang, T., Huang, L., Zhang, R., Gao, Y., Hu, D., Yu, S., et al. (2020). The impacts of climatic factors on radial growth patterns at different stem heights in Schrenk spruce (Picea schrenkiana). *Trees* 34, 163–175. doi: 10.1007/s00468-019-01908-4

Zhang, T., Wang, L., Yuan, Y., Wei, W., Yu, S., Zhang, R., et al. (2011a). A 645-year precipitation reconstruction in baluntai region on southern slope of mid-tianshan mountains based on tree-ring width. *Sci. Cientia Geograph. Sin.* 31, 251–256.

Zhang, T., Yuan, Y., Liu, Y., Wei, W., Zhang, R., Chen, F., et al. (2013). A tree-ring based temperature reconstruction for the Kaiduhe River watershed, northwestern China, since AD 1680: Linkages to the North Atlantic Oscillation. *Quaternary Int.* 311, 71–80. doi: 10.1016/j.quaint.2013.07.026

Zhang, T., Yuan, Y., Yu, S., Wei, W., Shang, H., Zhang, R., et al. (2011b). Contrastive analysis and climatic response of tree-ring gray values and tree-ring densities. *Acta Ecol. Sin.* 31, 6743–6752.

Zhang, X., Bai, X., Chang, Y., and Chen, Z. (2016). Increased sensitivity of Dahurian larch radial growth to summer temperature with the rapid warming in Northeast China. *Trees* 30, 1799–1806. doi: 10.1007/s00468-016-1413-6

Zhou, Z., Jiang, Y., Dong, M., Tao, Y., Wang, M., and Ding, X. (2018). Response of the relationship between radial growth and climatic factors to abrupt change of temperature along an altitudinal gradient on the northern slope of Changbai Mountain,Northeast China. *Acta Ecol. Sin.* 38, 4668–4676. doi: 10.5846/stxb201706171104

Zhu, J., and Zheng, J. (2022). Effects of diurnal asymmetric warming on terrestrial ecosystems. *Chin. J. Ecol.* 41, 777–783.